Journal of Solid State Chemistry 184 (2011) 825–829

Contents lists available at ScienceDirect

Journal of Solid State Chemistry

journal homepage: www.elsevier.com/locate/jssc

Synthesis, crystal structure and optical properties of a novel sodium lead pentaborate, $NaPbB_5O_9$

Min Zhang [a,b], Shilie Pan [a,*], Jian Han [a], Zhongxiang Zhou [a]

[a] Xinjiang Key Laboratory of Electronic Information Materials and Devices, Xinjiang Technical Institute of Physics & Chemistry, Chinese Academy of Sciences, Urumqi 830011, PR China
[b] Graduate University of Chinese Academy of Sciences, Beijing 100049, PR China

ARTICLE INFO

Article history:
Received 6 November 2010
Received in revised form
22 January 2011
Accepted 31 January 2011
Available online 4 February 2011

Keywords:
$NaPbB_5O_9$
Borate
Synthesis
Crystal structure

ABSTRACT

A novel sodium lead pentaborate, $NaPbB_5O_9$, has been successfully synthesized by standard solid-state reaction. The single-crystal X-ray structural analysis showed that $NaPbB_5O_9$ crystallizes in the monoclinic space group $P2_1/c$ with $a=6.5324(10)$ Å, $b=13.0234(2)$ Å, $c=8.5838(10)$ Å, $\beta=104.971(10)^\circ$, and $Z=4$. The crystal structure is composed of double ring $[B_5O_9]^{3-}$ units, $[PbO_7]$ and $[NaO_7]$ polyhedra. $[B_5O_9]^{3-}$ groups connect with each other forming two-dimensional infinite $_\infty[B_5O_9]^{3-}$ layers, while $[PbO_7]$ and $[NaO_7]$ polyhedra are located between the layers. $[PbO_7]$ polyhedra linked together via corner-sharing O atom forming novel infinite $_\infty[PbO_6]$ chains along the c axis. The thermal behavior, IR spectrum and the optical diffuse reflectance spectrum of $NaPbB_5O_9$ were reported.

1. Introduction

The crystal chemistry of metal borates, both as natural minerals and as synthetic materials with potentially useful physical properties ranging from nonlinear optical (NLO), ferroelectric, piezoelectric to semiconducting behaviors, is of continuing interest [1–3]. Moreover, anionic radicals in the borate class can be both B-tetrahedra and B-triangles, and the BO_3 and BO_4 groups may be further linked via common oxygen atoms to form isolated rings and cages or polymerize into infinite chains, layers and networks, leading to the rich structural chemistry [4,5]. Since a series of alkali-metal or alkaline-earth metal borate, such as LiB_3O_5 (LBO) [6], CsB_3O_5 (CBO) [7,8], $CsLiB_6O_{10}$ (CLBO) [9], β-BaB_2O_4 (BBO) [10] and $KBe_2BO_3F_2$ (KBBF) [11] are useful NLO materials for efficient SHG of Nd:YAG lasers, these induced a considerable interest in search for new promising compounds in ternary borate systems M_2O–$M'O$–B_2O_3 (M=alkali-metal and M'=Mg, Ca, Sr, Ba, Zn, and Cu) [12–21].

However, insofar as we know, there is no report on the mixed borates in M_2O–PbO–B_2O_3 (M=alkali-metal) systems until now. We have, therefore, started investigating these systems. The selection of lead borate for the investigation because of Pb^{2+} has $6s^2$ lone electron pairs and PbO_n groups have highly asymmetric bonding configuration, and some interesting materials may also be expected to exist in the Pb-containing borates. Extensive efforts in the ternary alkaline metal–lead–borate system led to a new phase, $NaPbB_5O_9$, which is the first borate discovered in the M_2O–PbO–B_2O_3 (M=alkali-metal) system. Herein we report synthesis, crystal structure, and optical properties of $NaPbB_5O_9$ for the first time.

2. Experimental

2.1. Compound synthesis

The title compound was synthesized by employing a conventional solid-state reaction method. All reagents were of analytical grade. Stoichiometric mixture of H_3BO_3 (3.092 g, 0.05 mol), PbO (2.232 g, 0.01 mol) and Na_2CO_3 (1.060 g, 0.01 mol) were mixed homogeneously and transferred to a Pt crucible. The sample was gradually heated to 630 °C, and kept at this temperature for 48 h with several intermediate grindings and mixings. X-ray powder diffraction data were collected using Bruker D2 PHASER diffractometer.

2.2. Thermal behavior analysis

The thermal behavior of $NaPbB_5O_9$ was investigated with the differential thermal analyses (DTA) using a NETZSCH STA 449C simultaneous thermal analyzer. The sample and reference Al_2O_3

---

* Corresponding author. Fax: +86 991 3838957.
E-mail address: slpan@ms.xjb.ac.cn (S. Pan).

0022-4596/$ - see front matter © 2011 Elsevier Inc. All rights reserved.
doi:10.1016/j.jssc.2011.01.039

were placed in a Pt crucible and heated at a rate of 10 °C/min in the range of 25–900 °C under flowing of nitrogen gas.

2.3. *Single crystal preparation*

H_3BO_3 (18.549 g, 0.3 mol), PbO (16.74 g, 0.075 mol), NaCl (4.383 g, 0.075 mol) and NaF (4.199 g, 0.1 mol) were precalcined at 300 °C for 2 h to decompose the boric acid, and the mixture was heated to 680 °C and kept for 10 h to ensure that the powder was melt completely in the solution and mixed homogeneously, then cooled down to 630 °C at a rate of 10 °C/h, and further to 600 °C at 0.5 °C/h, followed by cooling to room temperature at a rate of 20 °C/h. The colorless crystals with dimensions up to $0.5 \times 1.0 \times 1.0\ \mathrm{mm}^3$ were embedded in a borate matrix. Several small crystals could be isolated mechanically from the reaction product for the further characterization by single-crystal X-ray diffraction measurements.

2.4. *Structure determination*

Single-crystal XRD data were collected on a Bruker SMART APEX II 4 K CCD diffractometer at 296(2) K using Mo *Kα* radiation (λ=0.71073 Å) and integrated with a SAINT–*Plus* program [22]. The crystal structures were solved by direct methods and refined in SHELXTL system [23]. Final least-squares refinement on F_0^2 with data having $F_0^2 \geq 2\sigma(F_0^2)$ includes anisotropic displacement parameters for all atoms. Unit cell parameters were derived from a least-squares analysis of 6421 reflections in the range of 2.91–27.37°. The final difference Fourier synthesis map showed the maximum and minimum peaks at 1.112 and −0.915 e/Å^{-3}, respectively. The structure was checked for missing symmetry elements with *PLATON* [24]. Details of crystal parameters, data collection and structure refinements are given in Table 1, and the atomic coordinates and the equivalent isotropic displacement parameters are summarized in Table 2, and selected bond lengths and angles are listed in Table 3.

Table 1
Crystallographic data for $NaPbB_5O_9$.

Empirical formula	$NaPbB_5O_9$
Formula weight	428.23
Crystal system	Monoclinic
Space group	$P2_1/c$ (No. 14)
a (Å)	6.5324(10)
b (Å)	13.0234(2)
c (Å)	8.5838(10)
β (°)	104.971(10)
Volume (Å^3)	705.471(17)
Z	4
Density (calcd.) (g/cm^3)	4.032
Abs. coeff. (mm^{-1})	24.008
F(000)	760
Cryst size (mm^3)	$0.095 \times 0.104 \times 0.230$
The range for data collection (deg)	2.91–27.37
Index ranges	$-8 \leq h \leq 8,\ -16 \leq k \leq 16,\ -11 \leq l \leq 11$
Reflns collected/unique	6421/1604 [*R*(int)=0.0275]
Completeness to θ=27.37°	99.9%
data/restraints/param	1604/0/146
GOF on F^2	1.058
Final *R* indices [$F_0^2 > 2\sigma(F_0^2)$][a]	*R*1=0.0178, *wR*2=0.0444
R indices (all data) [a]	*R*1=0.0206, *wR*2=0.0455
Extinction coeff	0.0044(2)
Largest diff peak and hole (e/Å^3)	1.112 and −0.915

[a] $R_1=\Sigma||F_0|-|F_c||/\Sigma|F_0|$ and $wR_2=[\Sigma w(F_0^2-F_c^2)^2/\Sigma w\ F_0^4]^{1/2}$ for $F_0^2 > 2\sigma(F_0^2)$ and $w^{-1}=\sigma^2(F_0^2)+(0.0254P)^2+0.49P$ where $P=(F_0^2+2F_c^2)/3$.

Table 2
Atomic coordinates, equivalent isotropic displacement parameters and bond valence sum (BVS) for $NaPbB_5O_9$[a].

Atoms	*x*	*y*	*z*	U_{eq} (Å^2)	BVS
Na	0.5340(3)	0.4116(1)	0.8680(2)	0.019(1)	1.087
Pb	0.0908(1)	0.2884(1)	0.5577(1)	0.013(1)	2.033
B1	−0.4171(7)	0.2537(4)	0.6212(6)	0.010(1)	3.003
B2	0.0872(7)	0.0634(4)	0.3681(6)	0.012(1)	3.022
B3	−0.1637(7)	0.3882(3)	0.2285(6)	0.010(1)	3.023
B4	0.4525(7)	0.6508(3)	0.6436(6)	0.008(1)	3.033
B5	0.7912(7)	0.5515(4)	0.7503(6)	0.011(1)	3.029
O1	0.4912(4)	0.2431(2)	0.7470(4)	0.011(1)	2.048
O2	0.1630(5)	0.1536(2)	0.4290(4)	0.018(1)	2.007
O3	−0.2298(4)	0.3726(2)	0.3751(4)	0.009(1)	1.946
O4	0.5804(4)	0.5629(2)	0.7174(4)	0.011(1)	2.054
O5	−0.2521(5)	0.1919(2)	0.6052(4)	0.012(1)	2.042
O6	0.9280(4)	0.6254(2)	0.7260(4)	0.010(1)	2.092
O7	0.7742(4)	0.4881(2)	1.1530(4)	0.013(1)	2.057
O8	0.8697(4)	0.4572(2)	0.8176(4)	0.014(1)	2.044
O9	−0.5021(4)	0.3268(2)	0.5101(4)	0.010(1)	1.940

[a] U_{eq} is defined as one third of the trace of the orthogonalized U_{ij} tensor.

Table 3
Selected bond lengths (Å) and angles (deg) for $NaPbB_5O_9$[a].

Na–O7$^{\#1}$	2.368(3)	Pb–O2	2.190(3)
Na–O1	2.412(3)	Pb–O3	2.519(3)
Na–O8	2.417(3)	Pb–O6$^{\#5}$	2.656(3)
Na–O4	2.418(3)	Pb–O5	2.690(3)
Na–O5$^{\#2}$	2.539(4)	Pb–O1	2.763(3)
Na–O7	2.731(4)	Pb–O9	2.837(3)
Na–O2$^{\#3}$	2.743(3)	Pb–O6	2.844(3)
Mean	2.519	Mean	2.643
B1–O9	1.360(6)	O9–B1–O1$^{\#6}$	116.1(3)
B1–O1$^{\#6}$	1.371(5)	O5–B1–O9	121.8(4)
B1–O5	1.380(5)	O5–B1–O1$^{\#6}$	122.1(4)
Mean	1.371	Mean	120.0
B2–O2	1.329(5)	O7$^{\#8}$–B2–O8$^{\#7}$	118.1(4)
B2–O7$^{\#8}$	1.378(5)	O2–B2–O7$^{\#8}$	119.4(4)
B2–O8$^{\#7}$	1.400(5)	O2–B2–O8$^{\#7}$	122.4(4)
Mean	1.370	Mean	120.0
B3–O3	1.446(5)	O3–B3–O6$^{\#5}$	105.9(4)
B3–O7$^{\#10}$	1.463(5)	O5$^{\#9}$–B3–O6$^{\#5}$	106.6(3)
B3–O5$^{\#9}$	1.492(6)	O5$^{\#9}$–B3–O7$^{\#10}$	107.2(4)
B3–O6$^{\#5}$	1.498(5)	O6$^{\#5}$–B3–O7$^{\#10}$	111.6(3)
Mean	1.475	O3–B3–O5$^{\#9}$	111.8(3)
B4–O3$^{\#11}$	1.454(5)	O3–B3–O7$^{\#10}$	113.6(3)
B4–O4	1.462(5)	Mean	109.5
B4–O9$^{\#11}$	1.467(5)	O1$^{\#12}$–B4–O3$^{\#11}$	108.1(3)
B4–O1$^{\#12}$	1.511(5)	O4–B4–O9$^{\#11}$	108.1(3)
Mean	1.474	O1$^{\#12}$–B4–O9$^{\#11}$	109.0(3)
B5–O4	1.341(5)	O4–B4–O3$^{\#11}$	109.1(3)
B5–O6	1.365(5)	O4–B4–O1$^{\#12}$	109.5(4)
B5–O8	1.397(6)	O3$^{\#11}$–B4–O9$^{\#11}$	112.9(4)
Mean	1.368	Mean	109.5
		O4–B5–O8	115.6(4)
		O6–B5–O8	119.9(4)
		O4–B5–O6	124.5(4)
		Mean	120.0

[a] (#1) −*x*+1, −*y*+1, −*z*+2; (#2) *x*+1, −*y*+1/2, *z*+1/2; (#3) *x*, −*y*+1/2, *z*+1/2; (#4) *x*+1, *y*, *z*; (#5) −*x*+1, −*y*+1, −*z*+1; (#6) *x*−1,*y*,*z*; (#7) *x*−1, −*y*+1/2, *z*−1/2; (#8) −*x*+1, *y*−1/2, −*z*+3/2; (#9) *x*, −*y*+1/2, *z*−1/2; (#10) *x*−1, *y*, *z*−1; (#11) −*x*, −*y*+1, −*z*+1; and (#12) −*x*+1, *y*+1/2, −*z*+3/2.

2.5. *Vibrational spectroscopy and optical properties*

The infrared spectroscopy was carried out on a Shimadzu IRAffinity-1 spectrometer in order to specify and compare the coordination of boron in $NaPbB_5O_9$. The sample was mixed thoroughly with dried KBr (5 mg of the sample and 500 mg of KBr), and the spectrum was collected in the range from 400 to 4000 cm^{-1} with a resolution of 2 cm^{-1}.

UV–vis diffuse-reflectance data for $NaPbB_5O_9$ polycrystalline powder were collected at room temperature using a Shimadzu SolidSpec–3700DUV Spectrophotometer with the measurement range extending from 190 to 2600 nm.

3. Results and discussions

3.1. Synthesis and thermal behavior

Fig. 1 shows the observed powder XRD patterns of $NaPbB_5O_9$, together with calculated from the single crystal data for comparison. It is clear that the observed XRD patterns are in good agreement with the corresponding theoretical one, verifying the purity of synthesized powder sample is high. The XRD patterns also confirm our structural models correctly.

The thermal behavior of $NaPbB_5O_9$ is shown in Fig. 2. DTA curve shows one remarkable endothermic peak at 735 °C and there are two weak endothermic peaks at 765 and 830 °C, respectively, which indicates that $NaPbB_5O_9$ melts incongruently. Hence, flux method will be adopted to decrease melting temperature. After extensive attempts, NaF and NaCl were introduced into the system, and the small single crystals were obtained below 680 °C.

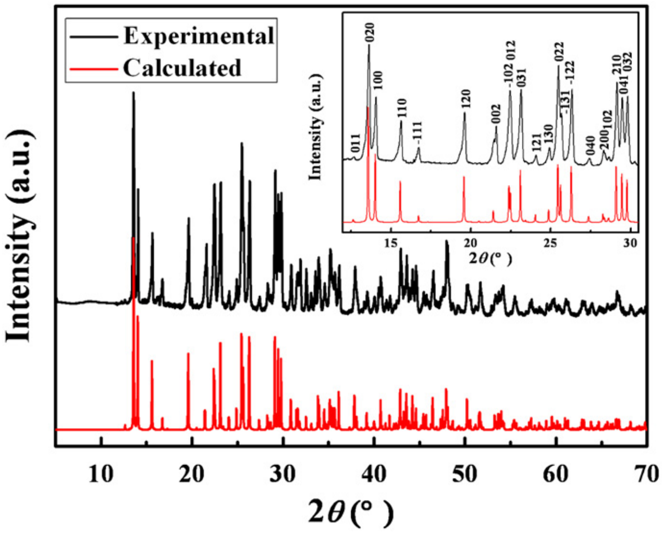

Fig. 1. Experimental and calculated XRD patterns of $NaPbB_5O_9$. Inset gives the XRD patterns in range of 10–30°.

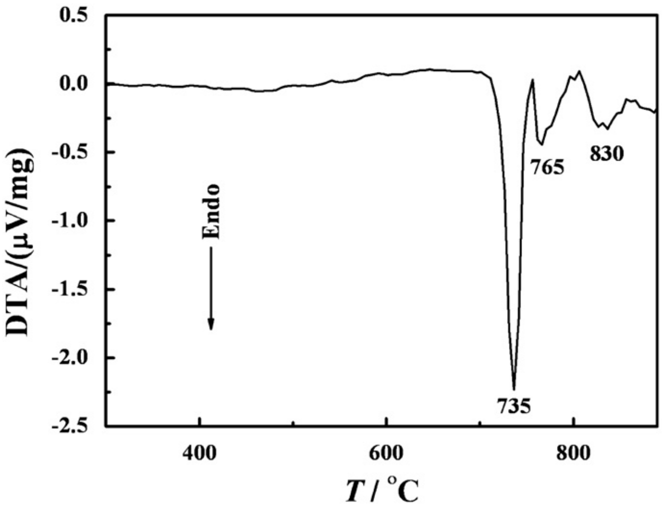

Fig. 2. DTA curve of $NaPbB_5O_9$.

3.2. Description of the structure

The X-ray diffraction has shown that the $NaPbB_5O_9$ crystallizes in a monoclinic space group $P2_1/c$. The crystal structure of $NaPbB_5O_9$ is schematically shown in Figs. 3 and 4 (the bonds of Pb–O and Na–O are removed for clarity). The basic structural unit in $NaPbB_5O_9$ is a $[B_5O_9]^{3-}$ group that consists of three BO_3 triangles (Δ) and two BO_4 tetrahedron ($\square$), which is condensed to a double ring via sharing the common tetrahedron. It can be written as $3\Delta2\square:\langle 2\Delta\square\rangle-\langle\Delta2\square\rangle$ with the help of the conception proposed by Burns et al. [25]. In this unit, two hexagonal rings are almost perpendicular to each other, and each $[B_5O_9]^{3-}$ group is vertex-linked to four other equivalent $[B_5O_9]^{3-}$ through its terminal O atoms to form a two-dimensional (2D) infinite corrugated ${}_{\infty}[B_5O_9]^{3-}$ layer extending in the (0 1 0) plane (Fig. 3). Na and Pb atoms are located between these layers to balance charge and also to hold the layers together through coordination with oxygen atoms (Fig. 4).

Selected bond lengths and angles for $NaPbB_5O_9$ are listed in Table 3, and each Na atoms is bonded to seven O atoms at distances of 2.368(3)–2.743(3) Å (average 2.519 Å). These results are very reasonable when compared with the ranges: 2.427(4)–2.577(5) Å (average 2.515 Å) in $K_2NaZnB_5O_{10}$ [26]; 2.218(2)–3.053(3) Å (average 2.517 Å) in $Na_3CaB_5O_{10}$ [13]; and 2.280(2)–3.084(3) Å (average 2.582 Å) in $Na_3ZnB_5O_{10}$ [14]. Bond valence sum (BVS) [27] calculation using Brown's formula for Na^+ is equal to 1.087 (Table 2), which further proves that the coordination of Na atoms are very reasonable.

Seven-coordinated Pb atoms is strongly bonded to one O atom (O2) at distance of 2.190(3) Å, and weakly bonded to six oxygens at distance of 2.519(3)–2.844(2) Å, therein six distant O atoms are provided by one ${}_{\infty}[B_5O_9]^{3-}$ layer and O2 is from neighboring layers. The average distance of Pb–O is 2.643 Å, which agrees well with those reported for the Pb^{2+} of the range 2.395(5)–2.894(4) Å (average 2.629 Å) in $Pb_2CuB_2O_6$ [28], and 2.364(6)–2.800(7) Å (average 2.476) in $Pb_2Cu_3B_4O_{11}$ [29]. The calculated BVS value of 2.033 for Pb^{2+} also verifies the coordination scheme.

The PbO_7 polyhedron is extremely distorted, because six oxygen neighbors located approximately on the same plane and only O2 almost perpendicular to the plane, leaving room for the

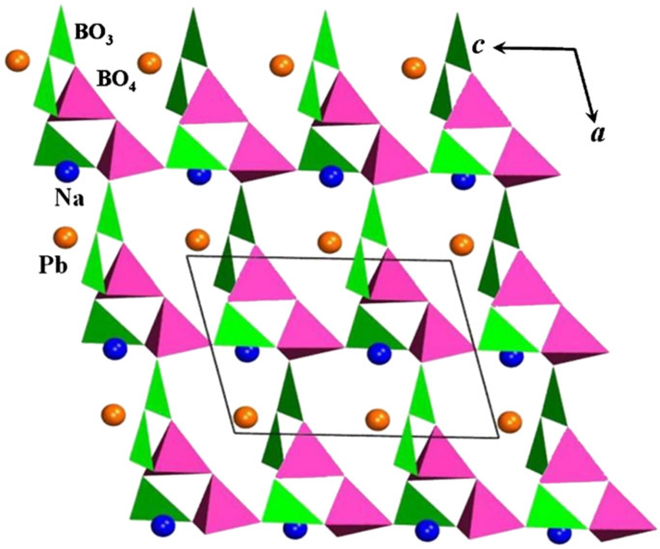

Fig. 3. Single ${}_{\infty}[B_5O_9]^{3-}$ layer parallel to the (0 1 0) plane in $NaPbB_5O_9$.

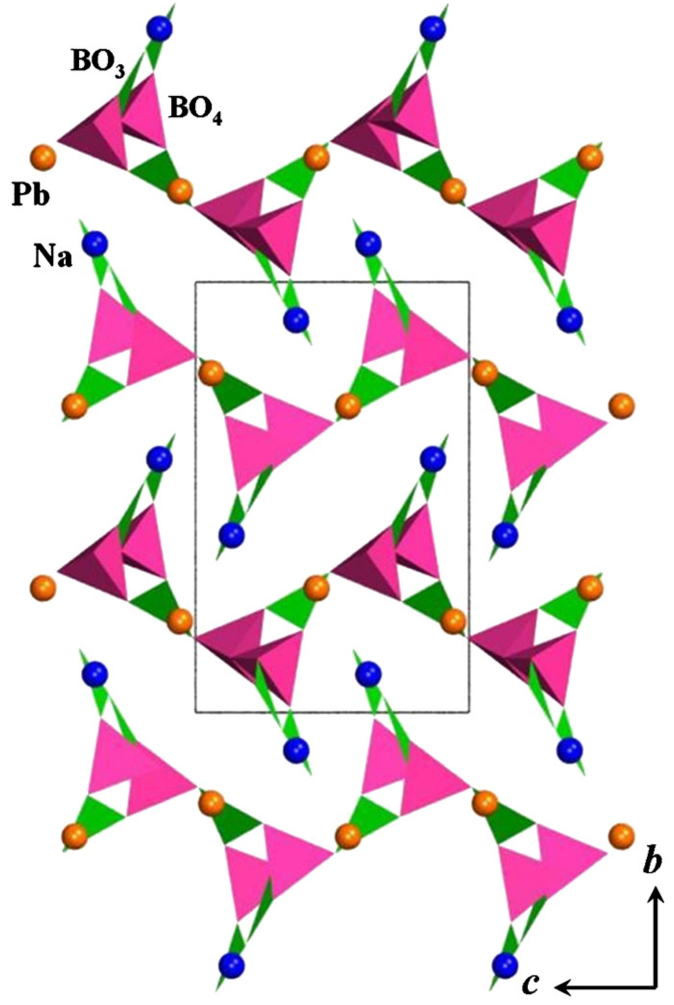

Fig. 4. Projection of $NaPbB_5O_9$ along the [100] direction.

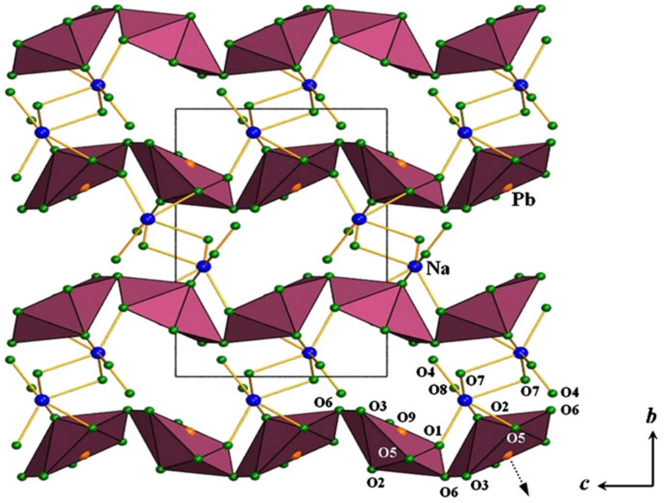

Fig. 5. Coordination geometry about the Pb atom and Na atom. Arrow indicates the direction of the electron lone pair of Pb atom.

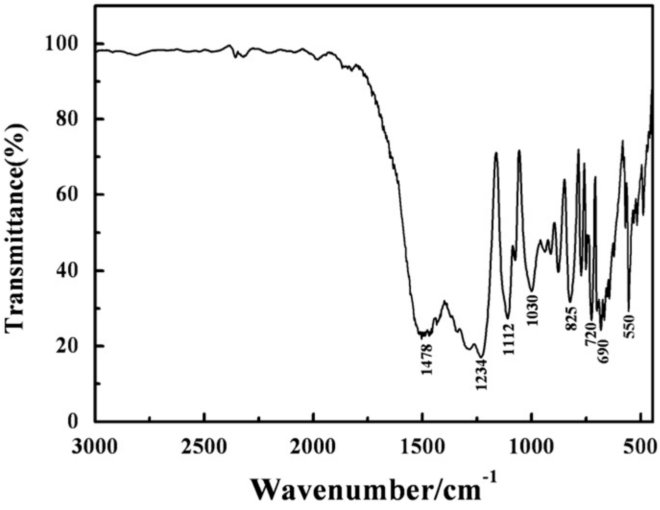

Fig. 6. Infrared spectrum of $NaPbB_5O_9$.

$6s^2$ lone pair of Pb^{2+} in the opposite direction to O2 (the direction of the electron lone pair of Pb atom is indicated by black arrow in Fig. 5). This configuration is very common for Pb^{2+}, as found in $PbBiBO_4$ [30]. In this structure, $[PbO_7]$ polyhedra linked together through two corner-sharing O atoms (O6) along the *c* axis to form infinite $_\infty[PbO_6]$ chains, while two $[NaO_7]$ polyhedra are joined by sharing edge to form an $[NaO_7]$ dimer, the dimers distributed between the $_\infty[PbO_6]$ chains and interconnected by sharing edges.

There are five crystallographically independent B atoms in the asymmetric unit, of which B1, B2, B5 atoms are in triangular coordination, B3 and B4 atoms are in tetrahedral coordination. The average B–O distances (Table 3) are very close to the data (1.370 and 1.476 Å, respectively) obtained for borate minerals by Hawthorne et al. [31], and the average O–B–O angles are equal to or slightly deviate from the ideal tetrahedral or triangular values (109.5° and 120°, respectively), indicating that the BO_4 and BO_3 groups are metrically regular. BVS for B atoms are also very reasonable, lying in the range of 3.003–3.033.

Three isostructural compounds of $NaPbB_5O_9$ have been reported in the literature, they are $NaCaB_5O_9$ [32], $NaSrB_5O_9$ [33] and $KSrB_5O_9$ [34]. All compounds crystallize in a monoclinic space group $P2_1/c$ and contain topologically identical $_\infty[B_5O_9]^{3-}$ layers. However, difference also exists, in the structures of $NaCaB_5O_9$, $NaSrB_5O_9$ and $KSrB_5O_9$, A^{2+} cations (A=Ca and Sr) coordinated with eight O atoms forming edge-sharing $_\infty[AO_8]$ chains, and the coordnation number of K or Na atoms is also eight. Whereas in the $NaPbB_5O_9$ structure, seven-coordinated Pb atoms form extremely distorted PbO_7 polyhedra, which are linked together by corner-sharing O atoms form $_\infty[PbO_6]$ chains, and Na atoms is also seven-coordinated. Due to the difference in radius and the coordination environments of metal cations, the coordinates of cations are slightly different from each other, such as the nearest distances between Na–Pb, Na–Sr, Na–Ca and K–Sr are 3.750, 3.719, 3.543 and 3.955 Å in $NaPbB_5O_9$, $NaSrB_5O_9$, $NaCaB_5O_9$ and $KSrB_5O_9$, respectively.

3.3. *Spectrum properties*

In order to further confirm the coordination of B atoms in $NaPbB_5O_9$ crystal structure, the infrared spectrum was measured (Fig. 6). The strong bands above 1112 cm^{-1} should be assigned to the BO_3 antisymmetric stretching vibrations, while those near 1030 cm^{-1} are mainly attributed to BO_4 antisymmetric stretch. The bands associated with BO_3 and BO_4 out of plane bending modes are overlapped and located at about 690–825 cm^{-1}. Bands with the frequencies below 550 cm^{-1} might be due to the Na–O and Pb–O vibrations, respectively. The IR spectrum further confirms the existence of both trigonally and tetrahedrally

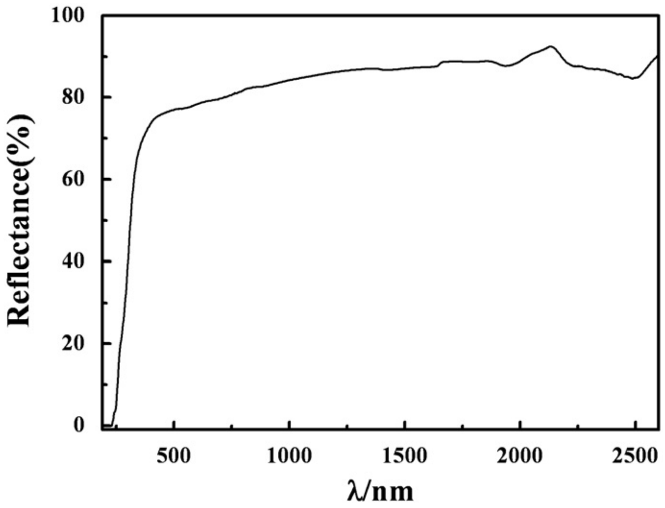

Fig. 7. UV–vis diffuse reflectance spectrum of $NaPbB_5O_9$.

coordinated boron atoms, consistent with the results obtained from the single-crystal X-ray structural analyses.

The optical diffuse reflectance spectrum is shown in Fig. 7. There are no absorption peaks above 420 nm, while absorption edge was observed at around 230 nm.

4. Conclusions

A novel ternary borate, $NaPbB_5O_9$ has been synthesized and single crystal X-ray diffraction reveals that interconnected $[B_5O_9]^{3-}$ groups form infinite layers along the (010) plane, and the NaO_7 and PbO_7 polyhedra distributed between the layers. IR spectrum and BVS calculation was used to verify the validity of the structure. $NaPbB_5O_9$, $NaCaB_5O_9$, $NaSrB_5O_9$ and $KSrB_5O_9$ are crystallized in monoclinic space group $P2_1/c$, and have the similar $_\infty[B_5O_9]^{3-}$ layers, whereas the coordinations of cations in $NaPbB_5O_9$ are different from the ones in other compounds.

Acknowledgments

We gratefully acknowledge the support from the “National Natural Science Foundation of China” (Grant nos. 50802110, 21001114), the “One Hundred Talents Project Foundation Program” of Chinese Academy of Sciences, the “Western Light Joint Scholar Foundation” Program of Chinese Academy of Sciences, the Natural Science Foundation of Xinjiang Uygur Autonomous Region of China (Grant nos. 200821159, 2009211B33), the “High Technology Research and Development Program” of Xinjiang Uygur Autonomous Region of China (Grant no. 200816120) and Scientific Research Program of Urumqi of China (Grant no. G09212001).

Appendix A. Supporting information

Supplementary data associated with this article can be found in the online version at doi:10.1016/j.jssc.2011.01.039.

References

[1] P. Becker, Adv. Mater. 10 (1998) 979.
[2] S.K. Filatov, R.S. Bubnova, Phys. Chem. Glasses 41 (2000) 216.
[3] H. Park, R. Lam, J.E. Greedan, J. Barbier, Chem. Mater. 15 (2003) 1703.
[4] S.L. Pan, J.P. Smit, M.R. Marvel, E.S. Stampler, J.M. Haag, J. Baek, P.S. Halasyamani, K.R. Poeppelmeier, J. Solid State Chem. 181 (2008) 2087.
[5] E.L. Belokoneva, Crystallogr. Rev. 11 (2005) 151.
[6] C.T. Chen, Y.C. Wu, A. Jiang, B.C. Wu, G. You, R.K. Li, S.J. Lin, J. Opt. Soc. Am., B 6 (1989) 616.
[7] L. Guo, G.L. Wang, H.B. Zhang, D.F. Cui, Y.C. Wu, L. Lu, J.Y. Zhang, J.Y. Huang, Z.Y. Xu, Appl. Phys. B 88 (2007) 197.
[8] Y.C. Wu, T. Sasaki, S. Nakai, A. Yokotani, H. Tang, C.T. Chen, Appl. Phys. Lett. 62 (1993) 2614.
[9] Y. Mori, I. Kuroda, S. Nakajima, T. Sasaki, S. Nakai, Appl. Phys. Lett. 67 (1995) 1818.
[10] C.T. Chen, B.C. Wu, A. Jiang, G. You, Sci. Sin. B 28 (1985) 235.
[11] B.C. Wu, D.Y. Tang, N. Ye, C.T. Chen, Opt. Mater. 5 (1996) 105.
[12] L. Wu, X.L. Chen, H. Li, M. He, Y.P. Xu, X.Z. Li, Inorg. Chem. 44 (2005) 6409.
[13] X.A. Chen, M. Li, J.L. Zuo, X.A. Chang, H.G. Zang, W.Q. Xiao, Solid State Sci. 9 (2007) 678.
[14] X.A. Chen, M. Li, X.A. Chang, H.G. Zang, W.Q. Xiao, J. Solid State Chem. 180 (2007) 1658.
[15] N. Penin, L. Seguin, M. Touboul, G. Nowogrocki, Int. J. Inorg. Mater. 3 (2001) 1015.
[16] G.J. Chen, Y.C. Wu, P.Z. Fu, J. Solid State Chem. 180 (2007) 2194.
[17] W.D. Cheng, H. Zhang, Q.S. Lin, F.K. Zheng, J.T. Chen, Chem. Mater. 13 (2001) 1841.
[18] L. Wu, X.L. Chen, H. Li, M. He, L. Dai, X.Z. Li, Y.P. Xu, J. Solid State Chem. 177 (2004) 1111.
[19] R. Norrestam, Z. Kristallogr. 187 (1989) 103.
[20] S.L. Pan, J.P. Smit, B. Watkins, M.R. Marvel, C.L. Stern, K.R. Poeppelmeier J. Am. Chem. Soc. 128 (2006) 11631.
[21] L. Wu, C. Wang, X.L. Chen, X.Z. Li, Y.P. Xu, Y.G. Cao, J. Solid State Chem. 177 (2004) 1847.
[22] SAINT, version 7.60A; Bruker Analytical X-ray Instruments, Inc.: Madison, WI, 2008.
[23] G.M. Sheldrick, SHELXTL, Version 6.14; Bruker Analytical X-ray Instruments, Inc.: Madison, WI, 2003.
[24] A.L. Spek, J. Appl. Crystallogr. 36 (2003) 7.
[25] P.C. Burns, J.D. Grice, F.C. Hawthorne, Can. Mineral 33 (1995) 1131.
[26] X.A. Chen, C.Y. Yang, X.A. Chang, H.G. Zang, W.Q. Xiao, J. Alloys Compd. 492 (2010) 543.
[27] I.D. Brown, D. Altermatt, Acta Crystallogr. B 41 (1985) 244.
[28] S.L. Pan, J.P. Smit, M.R. Marvel, C.L. Stern, B. Watkins, K.R. Poeppelmeier, Mater. Res. Bull. 41 (2006) 916.
[29] S.L. Pan, B. Watkins, J.P. Smit, M.R. Marvel, I. Saratovsky, K.R. Poeppelmeier, Inorg. Chem. 46 (2007) 3851.
[30] X.A. Chen, J.L. Zuo, X.A. Chang, Y.H. Zhao, H.G. Zang, W.Q. Xiao, J. Solid State Chem. 179 (2006) 3191.
[31] F.C. Hawthorne, P.C. Burns, J.D. Grice, Rev. Mineral. 33 (1996) 41.
[32] J. Fayos, R.A. Howie, F.P. Glasser, Acta Crystallogr. C 41 (1985) 1394.
[33] L. Wu, Y. Zhang, X.L. Chen, Y.F. Kong, T.Q. Sun, J.J. Xu, Y.P. Xu, J. Solid State Chem. 180 (2007) 1470.
[34] J.M. Tu, D.A. Keszler, Acta Crystallogr. C 51 (1995) 341.